Electrical Rectification in a Langmuir−Blodgett Monolayer of Dimethyanilinoazafullerene Sandwiched between Gold Electrodes

Robert M. Metzger,*,† Jeffrey W. Baldwin,† Walter J. Shumate,† Ian R. Peterson,† Prakash Mani,‡ Gary J. Mankey,‡ Todd Morris,§ Greg Szulczewski,§ Susanna Bosi,|| Maurizio Prato,|| Angelo Comito,⊥ and Yves Rubin⊥

Laboratory for Molecular Electronics of the Department of Chemistry, Department of Physics, and Department of Chemistry, Box 870336, The University of Alabama, Tuscaloosa, Alabama 35487-0336, Dipartimento di Scienze Farmaceutiche, Università di Trieste, Piazzale Europa 1, I-34127 Trieste, Italy, and Department of Chemistry and Biochemistry, University of California, Los Angeles, Box 951569, Los Angeles, California 90095-1569

Received: September 19, 2002

Asymmetries were observed across a monolayer of dimethylanilinoaza[C_{60}]fullerene, (DMA-NC_{60}, **1**) sandwiched between gold electrodes of relatively large size (0.265 mm^2). Two modes of behavior are observed: (1) a sigmoidal and slightly asymmetric behavior, bespeaking of a moderate unimolecular rectifier (rectification ratio of about 2), and (2) above a threshold voltage V_1 (≈0.6 to 1.0 V), a dramatic increase of current to 0.3 to 1 A (as high as 1.36×10^7 electrons $molecule^{-1}$ s^{-1} at 1.5 V), followed by ohmic behavior from V_1 to a relatively smaller negative bias V_2 (≈ −0.5 V to −0.6 V). At more negative potentials (e.g., at −1.5 V) the current is very small (a few μA). This high asymmetry in current persists for between 10 and 20 cycles of voltage scan. This increased, but ohmic conductivity is probably due to defects that grow at domain boundaries, since this behavior is not seen when very small electrodes (1 μm^2 area) are used. The defects could be stalagmitic filaments of gold which grow from the bottom electrode above V_1 but are broken at the negative bias V_2, or else they could be due to some unknown electrochemical couple. This device is vaguely reminiscent of Zener diodes or varistors: if operated between, say, + 2 V and −2 V, it is a super-rectifier, with a rectification ratio of up to 20 000 at 1.5 V.

Introduction

The Aviram-Ratner proposal[1] of a unimolecular electrical rectifier stimulated many experimental efforts,[2,3] which were finally successful,[4,5] and thoroughly confirmed.[6,7] The original proposal suggested a D−σ−A molecule connecting an electron donor moiety (D) to an electron acceptor moiety (A) through an insulating saturated "sigma" bridge σ;[1] the mechanism of action involves inelastic tunneling through the molecule from its first electronic excited-state $D^+-\sigma-A^-$ to the less polar ground-state $D^0-\sigma-A^0$.[2,3] The first confirmed rectifier was a ground-state zwitterion $D^+-\pi-A^-$, connected by a twisted π bridge, rather than a σ bridge, and used inelastic tunneling from the lower-polarity excited-state $D^0-\pi-A^0$ to the higher-polarity ground state.[6−8] It was also affected by the presence of a long aliphatic $C_{16}H_{33}$ chain, needed for LB film formation; such a chain, it should be noted, is absent in DMAn-NC_{60}, **1**. The molecule DMAn-NC_{60}, **1** (Figure 1), called "blue fullerene", was first synthesized at the University of California, Los Angeles, and studied for its nonlinear optical properties by hyper-Rayleigh scattering.[9]

Synthesis of DMAn-NC_{60}

The synthesis of DMAn-NC_{60}, **1**, is reported elsewhere.[9]

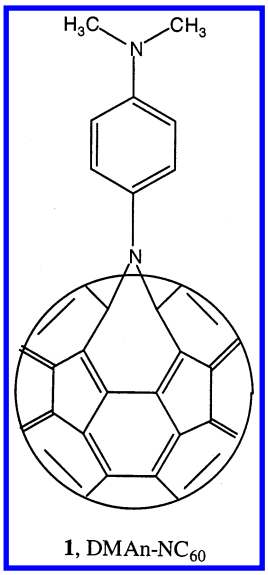

Figure 1. DMAn-NC_{60}, dimethylanilinoaza[C_{60}]fullerene, **1**.

Experimental Details

The molecules were used as received from the University of Trieste. Macroscopic current−voltage measurements were made on vacuum-annealed gold-coated substrates (Corning glass #1747F) prepared in an Edwards 306A evaporator at 7×10^{-6} mbar. Langmuir−Blodgett (LB) and Pockels-Langmuir (PL) films were studied using a PC-controlled Nima model 622D2 film trough, using 18 MΩ water (Millipore Milli-Q), connected

* Corresponding author.
† Laboratory for Molecular Electronics of the Department of Chemistry, The University of Alabama.
‡ Department of Physics, The University of Alabama.
§ Department of Chemistry, The University of Alabama.
|| Università di Trieste.
⊥ University of California.

10.1021/jp022101k CCC: $25.00
Published on Web 01/01/2003

to a constant-temperature bath (12.5 °C), in a temperature-controlled HEPA-filtered room (15.5 °C). The quality of the PL monolayer at the air−water interface was monitored by a Brewster angle microscope (MiniBAM, Nanofilm Technologies, Göttingen, Germany). Top gold electrodes were evaporated onto the sample, which was cooled by thermal contact to a coldfinger cooled with liquid nitrogen in an Edwards 306A evaporator, back-filled with Ar gas at 1×10^{-3} mbar, using a "cold gold" technique.[10,11] Current−voltage measurements were obtained using a PC-controlled (Labview) DC conductivity measuring system utilizing a Keithley 2400 SourceMeter that allows sourcing and measuring voltage from ±1 μV to ±200 V DC and current from ±10 pA to ±1 A.

A compact PL monolayer of DMAn-NC_{60} was formed by spreading a dilute (0.03 mg mL^{-1}) solution in chloroform on the air−water interface, and then decreasing the trough area (200 cm^2 min^{-1}). The PL monolayer at the air−water interface was transferred, on the upstroke at a constant pressure of 22 mN m^{-1} and at a rate of 25 mm min^{-1}, onto a freshly prepared hydrophilic gold-coated substrate, which was submerged in the subphase before spreading and compressing the monolayer.

LB monolayers of DMAn-NC_{60} on Au evaporated on a Si substrate were characterized using an X-ray Photoelectron Spectrometer (XPS, Kratos AXIS 165).

The valence-band molecular orbitals of DMAn-NC_{60} were computed using the PM3 algorithm of the program system HyperChem implemented on a PC microcomputer, with full geometry optimization.

Device Preparation

For electrical measurements, the LB monolayer film was dried in a vacuum desiccator with P_2O_5 for 3 days in the dark, prior to evaporating the top gold electrode. Because of the fragile nature of the monolayer, care was taken during the evaporation of the top Au electrode, to avoid damage to the film by thermal radiation or by collision with Au atoms of high kinetic energy.[11] The top gold electrode (estimated to be 17 nm thick from a similar evaporation [11]) was deposited by back-filling the chamber with Ar to a pressure of 1×10^{-3} mbar. The low-energy backscattered Au atoms were evaporated through a contact mask (0.28 mm^2) at a rate of 0.03 nm min^{-1}. The set of 50 metal−organic monolayer−metal (MOM) assemblies was removed from the vacuum system, and the conductivity of each MOM was characterized, using micromanipulators to make electrical contact in a shielded Faraday cage. Contact to the gold electrodes was achieved using a Ga/In eutectic (Alfa Aesar, 99.99%) connected to gold wires (Johnson Matthey, 99.998%, 0.05 mm diameter).

In a "small pads" experiment, a set of 16 very small Au pads (1 μm^2 in area) on Si, with fanout to contact pads, were coated with an LB monolayer, as above, then covered with a 17 nm thick Au electrode by the "cold gold" technique.[12] This preliminary "small pads" experiment produced "Au | monolayer | Au" pads with areas 280 000 times smaller than the "large pads", of area 0.265 mm^2 each, discussed above.

Results

The pressure−area isotherm is shown in Figure 2. Subsequent dilutions of the solution made no difference in the pressure−area isotherm. Higher temperatures moved the pressure onset to lower areas. Investigation of the film surface, using a Brewster angle microscope, shows a uniform but corrugated film coverage on the air−water interface. The measured areas are $A_o = 70$ Å^2 molecule^{-1} at zero pressure, and $A_c = 40$ Å^2 molecule^{-1} at the inflection point, i.e., at the collapse pressure of 50 mN m^{-1}, and $A_t = 50$ Å^2 at the transfer pressure of 22 mN m^{-1} (see below). If one estimates the C_{60} radius as 5 Å, then the calculated area of 78 Å^2 comes close to A_o. This is a lower calculated area than reported by others (98 Å^2),[14] yet experimental results have often given smaller areas than expected,[15−20] because of agglomeration of the C_{60} molecules into clusters even before films are spread,[19,21,22] except when dilution techniques were tried, which yielded $A_o = 96$ Å^2.[21,22] Dilution of the DMAn-NC_{60} dropping solution gave no increase in A_o.

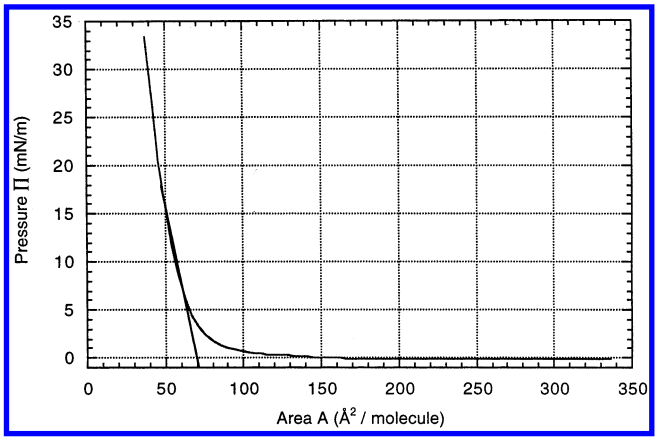

Figure 2. Pressure−area isotherm for DMAn-NC_{60}.

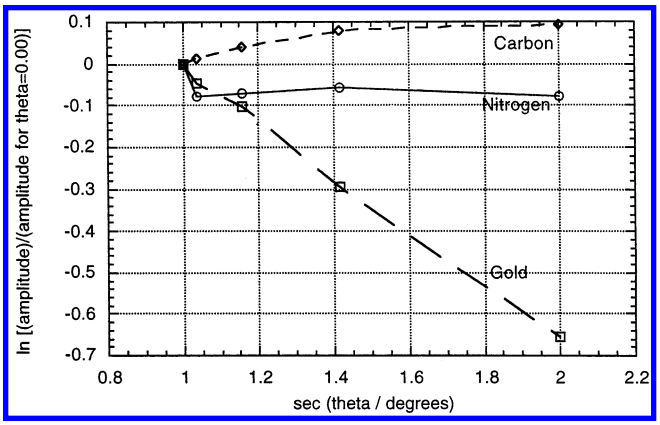

Figure 3. Plot of the natural logarithms of the Au 4f photoelectron current [ln(Au 4f amplitude divided by amplitude at zero degrees)], the C(1s) photocurrent, and the N(1s) photocurrent, as a function of sec θ, where θ is the takeoff angle. If the mean free path of the photoelectrons is 3.5 nm, then the thickness of the LB monolayer of DMAn-NC_{60} is 2.2 nm.

The XPS data for LB monolayers of DMAn-NC_{60}, transferred atop a 30 nm Au layer on a Si substrate, are shown in Figure 3. An XPS survey scan shows the presence of C, N, and Au, and Si. Furthermore, when the takeoff angle θ is varied, the intensity of Au 4f photoelectrons increases monotonically with takeoff angle, and has a maximum at normal incidence (θ = 90°): the electrons emitted from Au have maximum flux when they go through a minimum thickness of the organic monolayer. Figure 3 shows a plot of the natural logarithm of the Au 4f photoelectron flux, as a function of sec θ. If the mean free path of the Au 4f photoelectrons is taken to be 3.5 nm, then the thickness of the LB monolayer of DMAn-NC_{60} is 2.2 nm.

An analysis of the C, N, and Au core-level XPS data reveals (Figure 3) that there may be some organic carbonaceous adsorbate on the Au surface (since the photocurrent is independent of θ), covered by the LB monolayer of DMAn-NC_{60}; the angular dependence of the N(1s) signal at 401 eV suggests

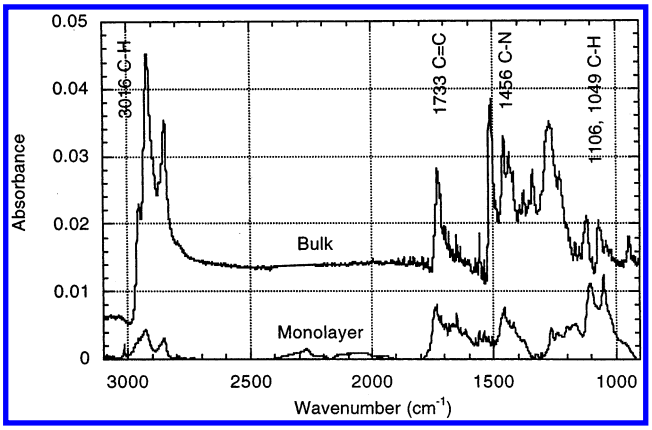

Figure 4. Top trace: bulk IR spectrum of DMAn-NC_{60} (NaCl plate, offset by 0.015 absorbance units). Bottom trace: RAIRS of monolayer of DMAn-NC_{60} (1000 scans, 4 cm^{-1} resolution) on gold substrate.

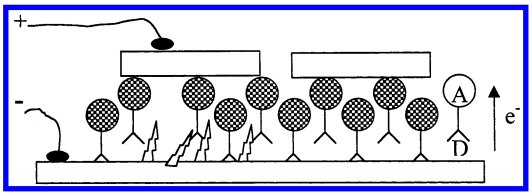

Figure 5. Schematic of monolayer of DMAn-NC_{60} on gold substrate. The electron donor (D) is the dimethylaniline ring; the electron acceptor moiety (A) is the azaC_{60}. The direction of preferred electron flow under forward bias is shown as an arrow from the bottom gold electrode to the top gold electrode pads. Also shown, as joined thunderbolts, are Au stalagmites that may grow from the bottom electrodes and may be the reason for the large currents observed for some pads.

that the dimethylaminophenyl and aza nitrogens are below the C_{60}, i.e., closer to the substrate.

Figure 3 shows there is no shift in the C(1s) signal as a function of the takeoff angle θ: the several contributors to the C(1s) spectrum (aromatic carbons, methyl carbons, fullerene carbons, adventitious layer carbons) which would be exposed differently at the various takeoff angles, could not be resolved in this experiment.

The reflection−absorption infrared spectrum (RAIRS) of DMAn-NC_{60} (bottom of Figure 4) shows the four anticipated C_{60} IR peaks (pure C_{60}: 528, 577, 1183, and 1429 cm^{-1} [23] and DMAn-NC_{60}: 472, 655, 1165, and 1435 cm^{-1}). The 472 and 655 cm^{-1} peaks are large ($A = 0.06$) and broad (the width at half-height is approximately 125 cm^{-1}), and are not shown in Figure 4, since they do not add to the interpretation of the orientation of the molecule. The aromatic C−H stretches (3016 cm^{-1}), the in-plane C−H bends (1049, 1106 cm^{-1}), and, most importantly, the C−N stretches of the tertiary amines (1456 cm^{-1}) are shown in the RAIRS and the bulk IR. These results and the surface selection rules imply that the plane of the dimethylaniline ring must not be oriented parallel to the plane of the substrate, but must be in a position either inclined or perpendicular to the surface plane.

We can now merge the film balance data, the theoretical molecular length, the XPS data, and the bulk IR and RAIRS data, and present a working model for the monolayer in Figure 5 (which also shows the bottom Au electrode, the top Au electrode, the direction of electron flow discussed below, and some "Au stalagmites", also discussed below).

We believe that the low area per molecule at transfer (A_t = 50 $Å^2$ at the transfer pressure of 22 mN m^{-1}, compared to a calculated molecular area of π $5.0^2 = 78$ $Å^2$) and the measured XPS film thickness of 2.2 nm (compared to a calculated length

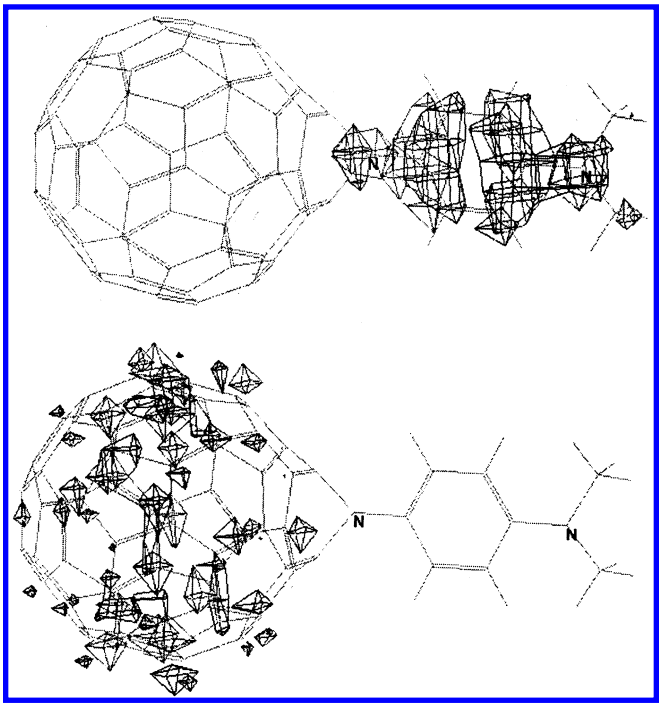

Figure 6. Computed (PM3) structure with (a) HOMO and (b) LUMO coefficients of DMAn-NC_{60}.

of 1.7 nm) both indicate an ultra-compact monolayer with slightly staggered molecules, as shown in Figure 5. The RAIRS data clearly show that the molecules must be oriented with a portion of the plane of the dimethylaniline ring inclined to, or perpendicular to, the surface plane, which is consistent with Figure 5.

What is not shown in Figure 5 is the possible 5 Å of organic aliphatic but hydrophilic contamination (aliphatic alcohols?) that may have accumulated on the native Au surface during its permanence under conductivity water before the LB monolayer was transferred to it. (This potential contaminant, in very small concentrations, may not have been removed by the ion-exchange and organic resin columns). If this 0.5 nm thick layer is present, then the DMAn-NC_{60} molecules need not be as staggered as shown in Figure 5.

The N 1s angle-resolved XPS data of Figure 3, and the direction of film transfer (on the upstroke, which is indicative of the hydrophilic dimethylamino group attaching itself to the bottom gold surface, which may be hydrophilic if still fresh) both support the orientation of the molecules shown in Figure 5.

Figure 6 shows the HOMO and LUMO amplitudes of DMAn-NC_{60}, computed by the PM3 algorithm using full geometry optimization. The data are summarized in Table 1. The computed ground-state dipole moment is 2.27 D. The five highest occupied molecular orbitals have energies, relative to the vacuum state, of −9.420, −9.408, −9.383, −9.259, and −8.384 eV (HOMO), respectively. The lowest unoccupied molecular orbitals have energies of −2.837 (LUMO), −2.812, −2.757 eV. Clearly, the 5-fold degeneracy of the HOMO in C_{60} (−9.482 eV) and the 3-fold degeneracy of the LUMO in C_{60} (−2.887 eV) are broken by the aza substituent. The HOMO is localized in the dimethylanilino ring (Figure 6b), while the LUMO is localized on the C_{60}, which is known to be an electron acceptor with electron affinity $E_A = -2.7 \pm 0.1$ eV,[24] similar to that of *p*-benzoquinone, a moderate electron acceptor. The auxiliary component molecules (**2** through **5**) mentioned in Table

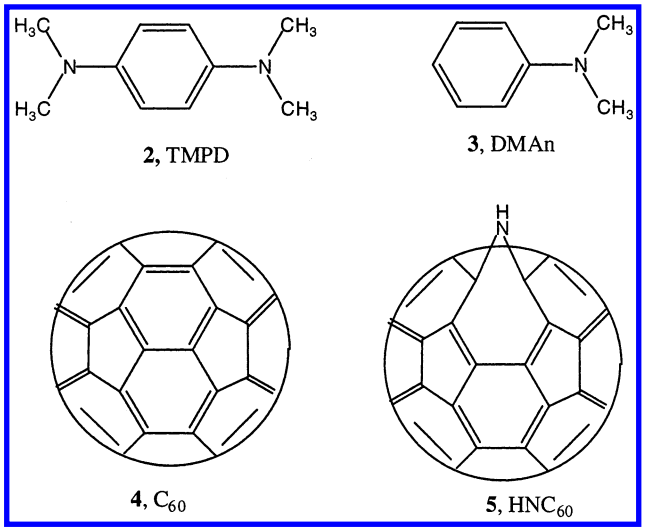

Figure 7. Molecular structure of molecules **2** through **5**.

TABLE 1: Molecular Orbital Calculations (PM3, with geometry optimization, using HyperChem) of DMAn-NC_{60} and Its Constituent Donor and Acceptor Moieties[a] [a]B.E. = binding energy, ΔH_f = Heat of Formation, μ = Dipole Moment)

structure	TMPD **2**	DMAn **3**	C_{60} **4**	HNC_{60} **5**	DMAn-NC_{60} **1**
B.E.(kcal/mol)	−2752.	−2033.	−9,442.7	−9,601.7	−11,523.
ΔH_f (kcal/mol)	16.6	19.77	810.7	816.8	844.1
μ (D)	0.04	1.18	0.00	1.04	2.27
HOMO-4 (eV)	−11.680	−12.673	−9.482	−9.553	−9.420
HOMO-3 (eV)	−10.840	−11.927	−9.482	−9.471	−9.408
HOMO-2 (eV)	−9.705	−10.500	−9.482	−9.456	−9.383
HOMO-1 (eV)	−9.282	−9.713	−9.482	−9.430	−9.259
HOMO (eV)	−7.926	−8.449	−9.482	−9.282	−8.384
LUMO (eV)	0.478	0.452	−2.887	−2.884	−2.837
LUMO+1 (eV)	0.529	0.486	−2.887	−2.860	−2.812
LUMO+2 (eV)	2.258	2.195	−2.887	−2.791	−2.757

1 have the structures given in Figure 7. As mentioned above, the computed molecular length of DMAn-NC_{60} (Figure 6) is about 17 Å.

It is quite remarkable that the computed LUMO level of DMAn-NC_{60} (−2.837 eV) is so close to that of underivatized C_{60}, while the HOMO of DMAn-NC_{60} (−8.384 eV) is very close to that of DMA (−8.449 eV), but not close to that of TMPD (−7.926 eV): the computed dipole moment of DMAn-NC_{60} is low (2.27 D), consistent with a coupling of a weak donor (DMA) with a moderate acceptor (C_{60}).

The UV−vis spectrum of DMAn-NC_{60} in tetrahydrofuran (Figure 8) shows an intervalence transfer (IVT) band peak at about 720 nm (1.66 eV), which usually is assumed to be close to the band gap. This contrasts with a large calculated HOMO−LUMO gap of 8.384 − 2.837 eV = 5.547 eV.

Figure 9 shows the X-ray reflectivity of the monolayer of DMAn-NC_{60} on a gold−Ti−SiO_x−Si substrate. The most notable feature of the $\theta-2\theta$ scan is the Kiessig fringes, which are due to reflection of X-rays from the top of the gold surface (LB film−gold interface) to the bottom of the gold surface (gold−titanium interface). These data were collected, and after deconvolution yield the electron density and electron density plots of Figure 10, from which details about the monolayer structure may be determined.

Rectification

Having dispensed with structural considerations, we can now present the $I-V$ data. Each MOM assembly was measured separately. Of these, 10% were short circuits, mainly due to

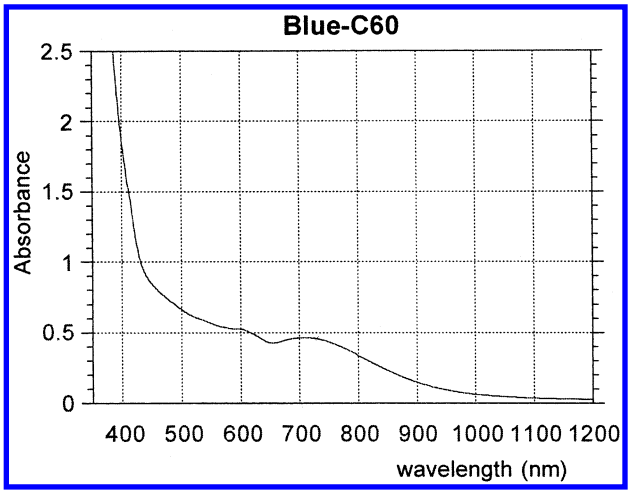

Figure 8. UV−vis spectrum of a solution of DMAn-NC_{60} in tetrahydrofuran.

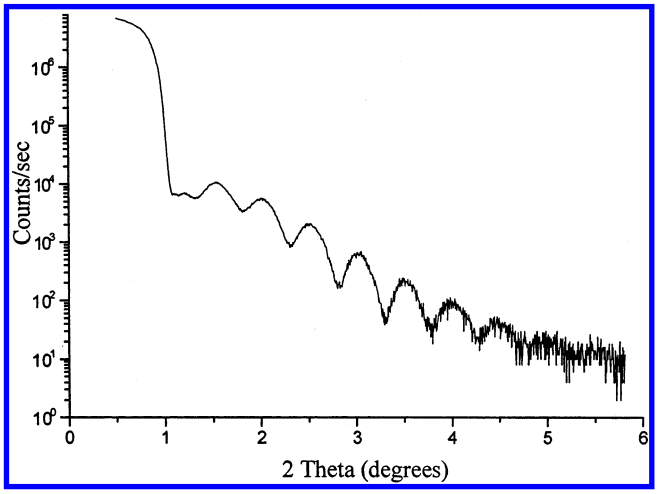

Figure 9. The X-ray reflectivity of a monolayer of DMAn-NC_{60} on gold−Ti−SiO_x−Si substrate shows Kiessig fringes from gold substrate.

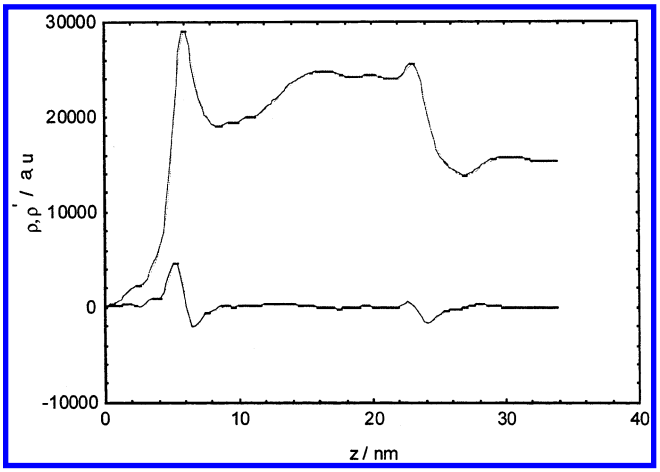

Figure 10. Electron density (top) and electron density gradient (bottom) from X-ray reflectivity of a monolayer of DMAn-NC_{60} on gold−Ti−SiO_x−Si substrate.

the inability to control the thickness of the top gold electrode, or due to imperfections in the LB film. When the top gold electrode is too thin, there is uneven coverage of the surface, because at low coverage gold tends to first form microscopic gold spheres, which unevenly coat the surface,[26] so that electrical shorts develop to the bottom electrode. The remaining 90% of the MOM assemblies had DC resistances of 2 Ω at positive

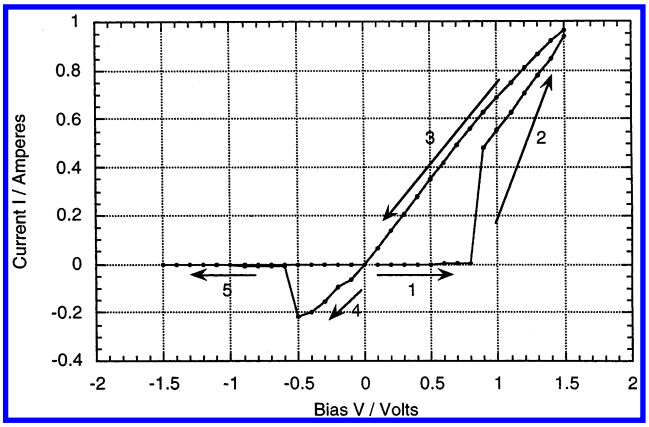

Figure 11. $I-V$ curve for a monolayer of DMAn-NC_{60} between two gold electrodes (bias range −1.5 V to + 1.5 V and back to −1.5 V, with direction of voltage scan indicated by successive integers and arrows. The large currents are probably due to extrinsic effects, not the monolayer.

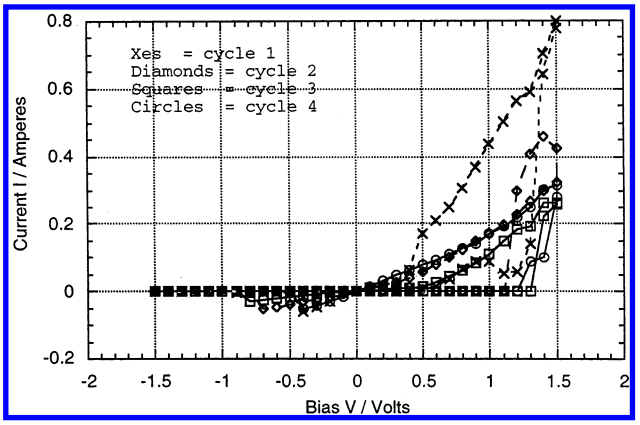

Figure 12. $I-V$ curves of monolayer of DMAn-NC_{60} between gold electrodes; successive scans are indicated by the symbols: X's or crosses (X), diamonds (◇), squares (□), and circles (○). Bias applied: −1.5 V to 1.5 V and back to −1.5 V. The large currents are probably due to extrinsic effects, not the monolayer.

bias to 75 kΩ at negative bias; and of these, all had rectifying behavior, i.e., none had symmetrical $I-V$ curves. In contrast to a previous study,[13] no reverse rectification was seen for any pad. The rectification ratio (RR) is defined as:

$$\mathrm{RR}(V_o) = |\ \text{Current at } V_o\ |/|\ \text{Current at } -V_o\ | \qquad (1)$$

If one looks only at the magnitudes of the observed asymmetries, the rectification ratios seen for many pads average an incredible 12000 ± 2000 at ±1.5 V, which corresponds to a field of approximately 1 GV m^{-1} and a current density of 300 A cm^{-2}, or, using a molecular area of 70 $Å^2$, a massive 1.36×10^7 electrons $molecule^{-1}$ s^{-1}. Repeated measurement of the same MOM leads to increasing RR, but decreasing currents, so that the $I-V$ asymmetry decreases after approximately 15 cycles. However, it is very noteworthy that the initial asymmetry returns if the structure is left at zero voltage for a period of fifteen to thirty minutes, and is then remeasured.

Figure 11 shows an $I-V$ curve for a monolayer of DMAn-NC_{60} between two gold electrodes, with the bias scan range 1.5 V to −1.5 V. Above a threshold voltage (V_1), the monolayer shows dramatically higher currents at positive bias, than for the corresponding negative bias. V_1 varies, from junction to junction, in the range 0.6 to 1.2 V. Under positive bias, the easy-current direction, the top electrode is positive and electrons flow from the bottom electrode to the top electrode, as shown in Figure 5.

The interesting result is that, once the bias is above V_1, the current I greatly increases with voltage, but remains ohmic (i.e., I is linear with V) as the bias is reversed (arrows 3 and 4 in Figure 11), to a negative bias V_2 (which is smaller in magnitude than V_1). This ohmic behavior suggests metallic behavior, rather than tunneling behavior. If the bias is more negative than V_2, the current drops dramatically.

We believe that on the scan from −1.5 V to V_1 (from arrow 5 to 1 in Figure 11), the behavior is that of an organic material, with low currents and a sigmoidal shape. The region of arrow 2 in Figure 11 is a mixture of filamentary and organic conduction. The region of arrows 3 and 4 in Figure 11 is pure filamentary conduction until it reaches a negative potential V_2, at which (arrow 5 in Figure 11) it again conducts through the organic film. Filamentary behavior has been studied by others[27] and reported to cause symmetrical $I-V$ characteristics.[28] Also, gold clusters (2−5 nm in size) are known to form under potential within the LB film at the gold−LB film interface, and they have shown coulomb charging phenomena, but with symmetrical $I-V$ curves.[26] The behavior of four successive cycles for a different pad is shown in Figure 12.

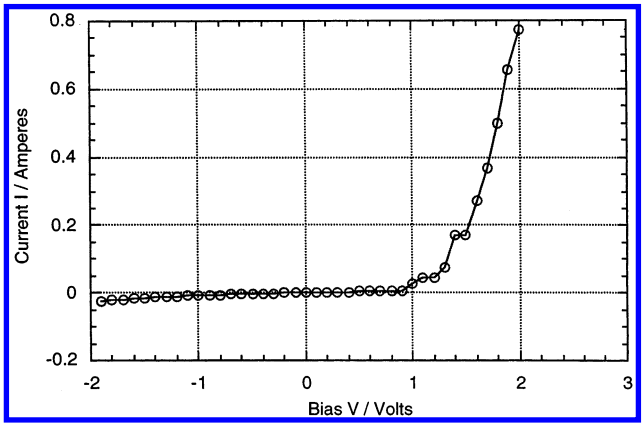

Figure 13. $I-V$ curve of DMAn-NC_{60} monolayer between Au electrodes (bias −2 to +2 V). The large currents are probably due to extrinsic effects, not the monolayer.

Figure 13 shows a pad studied between −2.0 V and +2.0 V, but with no measurements from positive bias to negative bias. This time, the threshold potential V_1 is about 1.2 V, as it is for Figure 12. The variation of V_1 with MOM pad has been seen before.[6,13]

A preliminary "small pads" experiment (area 1 μm^2 each) yielded $I-V$ curves with no trace of the large currents seen for the "large" pads (area 0.265 mm^2 each) in Figure 11, Figure 12, and Figure 13.[12] This finding suggests that the large forward currents in Figure 11, Figure 12, and Figure 13 are due to defects, whose number must be much larger in the large pads.

A different behavior can be seen for some pads, in which large currents are NOT observed (Figure 14): the $I-V$ curve is sigmoidal, but mildly asymmetric, with a RR of about 2, which is marginally rectifying.[13] No evidence of large currents or ohmic behavior is observed, which is one reason we claim that this is due to conduction through the organic monolayer without metallic filaments.

The other reason is that the $I-V$ curves shown in Figure 14, as well as a third pad from a different sample, all show excellent fits to the equation of elastic charge transport through a single molecule:[29]

$$I = (2I_o/\pi)\{\tan^{-1}[\theta^{-1}(pV - V_o)] - \tan^{-1}[\theta^{--1}((1-p)V + V_o)]\} \qquad (2)$$

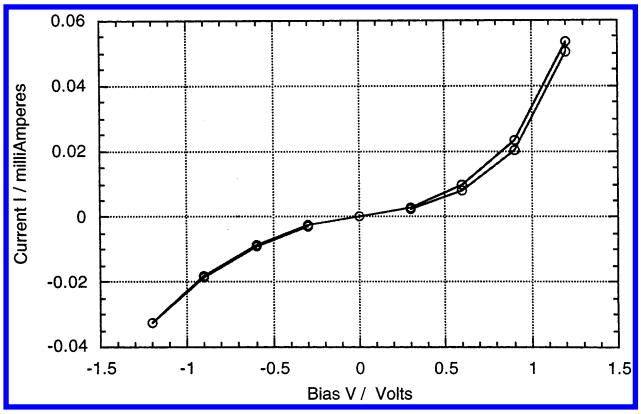

Figure 14. *I*−*V* curve of DMAn-NC_{60} monolayer between Au electrodes (bias −1.3 to +1.3 V). Low currents and small asymmetry are due to the organic monolayer.

TABLE 2: Fit of *I*−*V* Curves of Figure 14, and of Two More Pads (not shown) to Equation $I = I\,[\tan^{-1}(b + cV) - \tan^{-1}(b - dV)]$, *I* = Current Prefactor (mA)[a]

pad no.	b	c	d	I	p	w	V_o	A
1	4.255	3.083	3.552	0.03567	0.465	0.151	0.64	19.09
2	3.393	3.217	3.858	0.02394	0.455	0.141	0.62	19.42
3	2.294	1.707	1.776	0.03238	0.490	0.287	0.66	19.83

[a] The corresponding derived quantities (from eq 2) are the following: $w = 1/(c + d)$ = Lorentzian half width at half amplitude, $V_o = b/(c + d)$ = potential of alignment (volts), $p = c/(c + d)$ = center of gravity of rectifying unit within gap, $A = \log(I/Q\ w\ N)$ = attenuation (nepers), where $Q = 7.5 \times 10^{-5}$ Siemens = quantum of conductance, N = pad area/area per molecule = 0.285 mm^2/70 $Å^2$ = 3.36×10^{11} molecules/pad.

where the current I is a function of voltage V, I_o is the saturation (or plateau) current, θ is the tunneling gap coupling parameter, $e\ V_o$ is the zero-bias energy difference between the dominant level and the Fermi level, and the parameter p gives the fractional position of the "center of gravity" of the molecular energy level used in charge transport within the electrode gap.[29] A simplified version of this elastic charge transport equation, $I = i\ \tan^{-1}(b + cV) - \tan^{-1}(b - dV)$ was used in order to perform a curve-fit using the program Easy Plot. The results are given in Table 2. The good fit strongly suggests that the conduction is indeed due to current through the molecule, as seen previously for the unimolecular rectifier hexadecylquinolinium tricyanoquinodimethanide.[11]

The absence of an aliphatic chain in this LB film-forming molecule is significant, and is reflected in the attenuation values. The molecule should have a low degree of flexibility, and should not have the problem associated with low-conducting alkyl chains, which tend to undergo damage due to hot electrons under applied potential.[30] In fact, the rectification ratios have been seen to reverse in monolayers of those molecular rectifiers which contain alkyl chains, which is consistent with the damage due to hot electrons.[30] Thus, for DMAn-NC_{60} we have no evidence of flipping, and have seen no evidence of reverse rectification curves due to molecular reorientation. Also, the alkyl (saturated) molecules have been known for a long time to be more resistive than aromatic molecules.[31] Higher currents in these structures persist, due to the absence of alkyl groups.

Discussion

The film thickness measured by XPS (2.2 nm) can receive a contribution of about 0.5 nm from adventitious carbonaceous material that may have been formed atop the Au electrode, and below the LB monolayer, because of soluble hydrocarbon species dissolved even in the water of highest possible purity available.[32] If this layer does exist, then the arguments leading to the slightly staggered arrangement of the molecules in Figure 5 are weakened, as mentioned above.

The very large forward currents and very small currents at reverse bias, and therefore the impressively large rectification ratios, are due to either asymmetric tunneling through an ordered monolayer, or are due to the formation of filaments of Au that are interspersed between the dimethylanilino groups of adjacent molecules, most likely the latter (Figure 5). The asymmetry of the *I*−*V* curves clearly indicates that such filaments do not occur with equal frequency on the two sides of the monolayer: they seem to be stalagmites, rising from the bulk metal Au bottom electrode, rather than stalactites, descending from the thin top pads. These filaments would discharge electrons preferentially from their tips across whatever part of the monolayer is still intact, to the other electrode. If the filaments extended all the way across the monolayer, and were macroscopically thick, then short circuits of very low resistance ($\mu\Omega$ to mΩ) would be expected. If the filaments were true nanowires, one or three atoms across, the quantum of resistance of 12.6 kΩ per nanowire would be expected, or 12.6/N kΩ for N nanowires in parallel. The two-probe measurements performed here give an overall resistance for path 3 in Figure 13 of about 1 Ω (including all contact resistances in series). We seem to be in some intermediate regime, which suggests that the nanowires and part of the monolayer are together involved in the conduction process (e.g., Au nanowire to C_{60}).

It is significant that when two different pads, which initially showed characteristics similar to Figure 13, were cycled twenty or forty times, respectively, between +1.5 V and −1.5 V, then the large currents seen in Figure 11 would be replaced by the much smaller currents seen in Figure 14: somehow the Au filaments would be destroyed, and the sigmoidal behavior of the organic monolayer would be the "steady-state" behavior of the MOM.

In a preliminary "small pads" experiment, the large forward currents of Figure 11, Figure 12, or Figure 13 were not seen.[12] This finding reinforces the notion that the large forward currents are due to defects, whose number is much larger in the large pads (area 0.265 mm^2 each) than in the small pads (1 μm^2 each).

Acknowledgment. We are grateful to Dr. Paul L. Evans of the University of Alabama for collecting the X-ray reflectivity data. This work was supported at the University of Alabama by National Science Foundation Grant DMR-FRG-00-95215 "Oligomolecular Nanodevices", and at the University of Trieste by MURST (cofin prot. MM03198284), by C.N.R. through the program "Materiali Innovativi (legge 95/95)"

References and Notes

(1) Aviram, A.; Ratner, M. A. *Chem. Phys. Lett.* **1974**, *29*, 277−283.

(2) Metzger, R. M.; Panetta, C. A. *New J. Chem.* **1991**, *15*, 209−221.

(3) Metzger, R. M. In *Molecular and Biomolecular Electronics*; Birge, R. R., Ed.; *ACS Adv. Chem. Ser. 240* (American Chemical Society: Washington, DC, 1994; pp 81−129.

(4) Ashwell, G. J.; Sambles, J. R.; Martin, A. S.; Parker, W. G.; Szablewski, M. *J. Chem. Soc., Chem. Commun.* **1990**, 1374−1376.

(5) Martin, A. S.; Sambles, J. R.; Ashwell, G. J. *Phys. Rev. Lett.* **1993**, *70*, 218−221.

(6) Metzger, R. M.; Chen, B.; Hopfner, U.; Lakshmikantham, M. V.; Vuillaume, D.; Kawai, T.; Wu, X.; Tachibana, H.; Hughes, T. V.; Sakurai, H.; Baldwin, J. W.; Hosch, C.; Cava, M. P.; Brehmer, L.; Ashwell, G. J. *J. Am. Chem. Soc.* **1997**, *119*, 10455−10466.

(7) Metzger, R. M. *Acc. Chem. Res.* **1999**, *32*, 950−957.

(8) Baldwin, J. W.; Chen, B.; Street, S. C.; Konovalov, V. V.; Sakurai, H.; Hughes, T. V.; Simpson, C. S.; Lakshmikantham, M. V.; Cava, M. P.; Kispert, L. D.; Metzger, R. M. *J. Phys. Chem B* **1999**, *103*, 4269−4277.

(9) Comito, A.; Schick, G.; Viado, A. L.; Asselberghs, I.; Bartberger, M. D.; Khan, S. I.; Houk, K. N.; Clays, K.; Rubin, Y. *J. Am. Chem. Soc.*, submitted.

(10) Okazaki, N.; Sambles, J. R. "A New Fabrication Technique and Current−Voltage Properties of an Au/LB/Au Structure", *International Symposium on Organic Molecular Electronics, Nagoya, Japan, May 18, 2000;* pp 66−67.

(11) Metzger, R. M.; Xu, T.; Peterson, I. R, *J. Phys. Chem. B* **2001**, *105*, 7280−7290.

(12) Xu, T.; Jaiswal, A.; Reed, M. A. Metzger, R. M. Unpublished results.

(13) Vuillaume, D.; Chen, B.; Metzger, R. M. *Langmuir* **1999**, *15*, 4011−4017.

(14) Milliken, J.; Dominguesz, D. D.; Nelson, H. H.; Barger, W. R. *Chem Mater*. **1992**, *4*, 252−254.

(15) Obeng, Y. S.; Bard, A. J. *J. Am. Chem. Soc.* **1991**, *113*, 6279−6280.

(16) Long, C.; Xu, Y.; Gou, F.; Li, F.; Xu, D.; Yao, Y.; Zhu, D. *Solid State Commun.* **1992**, *82*, 381−383.

(17) Nakamura, T.; Tachibana, H.; Yumura, M.; Matsumoto, M.; Azumi, R.; Tanaka, M.; Kawabata, Y. *Langmuir* **1992**, *8*, 4−6.

(18) Williams, G.; Pearson, C.; Bryce, M. R.; Petty, M. C. *Thin Solid Films* **1992**, *209*, 150−152.

(19) Wang, P.; Shamsuzzoha, M.; Wu, X.-L.; Lee, W.-J.; Metzger, R. M. *J. Phys. Chem.* **1992**, *96*, 9025−9028.

(20) Wang, P.; Chen, B.; Metzger, R. M.; Da Ros, T.; Prato, M. *J. Mater. Chem.* **1997**, *7*, 2397−2400.

(21) Bulhões, L. O. S.; Obeng, Y. S.; Bard, A. J. *Chem. Mater*. **1993**, *5*, 110−114.

(22) Wang, P.; Maruyama, Y.; Metzger, R. M. *Langmuir* **1996**, *12*, 3932−3937.

(23) Fabian, J. *Phys Rev. B* **1996**, *53*, 13864−13870.

(24) Wang, L. S.; Conceicao, J.; Jin, C.; Smalley, R. E. *Chem. Phys. Lett.* **1991**, *182*, 5.

(25) Chlistunoff, J.; Cliffel, D.; Bard, A. J. *Thin Solid Films* **1995**, *257*, 166−184.

(26) Philipp, G.; Muller-Schwanneke, C.; Burghard, M.; Roth, S.; v. Klitzing, K. *J. Appl. Phys.* **1999**, *85*, 3374−3376.

(27) Peterson, I. R. *J. Chim. Phys.* **1988**, *85*, 997−1001.

(28) Couch, N. R.; Montgomery, C. M.; Jones, R. *Thin Solid Films* **1986**, *135*, 173−186.

(29) Peterson, I. R.; Vuillaume, D.; Metzger, R. M. *J. Phys. Chem. A* **2001**, *105*, 4702−4707.

(30) Steitz, R.; Peterson, I. R. In *Electron Crystallography of Organic Molecules*; Fryer, J. R., Dorset, D. L., Eds.; NATO ASI **C328**; Kluwer: Dordrecht, 1990; pp 365−375.

(31) Bumm, L. A.; Arnold, J. J.; Cygan, M. T.; Dunbar, T. D.; Burgin, T. P.; Jones, L., II.; Allara, D. L.; Tour, J. M.; Weiss, P. S. *Science* **1996**, *271*, 1705−1707.

(32) Peterson, I. R. Unpublished results.